On punctate white matter lesions in preterm infants: Is ultrasound diagnosis feasible?

Philippe Quétin, Nicolas Leboucq, Charlotte Boyer, Françoise Crozier, Philippe Delachartre, Marilyne Grinand, Philippe Masson, Olivier Claris

On punctate white matter lesions in preterm infants: Is ultrasound diagnosis feasible?

Philippe Quétin [a,*], Nicolas Leboucq [b], Charlotte Boyer [b], Françoise Crozier [a], Philippe Delachartre [c], Marilyne Grinand [d], Philippe Masson [a], Olivier Claris [e,f,g]

[a] Service de Néonatalogie, Centre Hospitalier Henri Duffaut, Avignon, France
[b] Unité d'Imagerie Pédiatrique, CHU Arnaud de Villeneuve, Montpellier, France
[c] Univ Lyon, INSA-Lyon, Université Claude Bernard Lyon 1, UJM-Saint Etienne, CNRS, Inserm, CREATIS, UMR 5220, U1294, Lyon, France
[d] Unité de Recherche Clinique, Centre Hospitalier Henri Duffaut, Avignon, France
[e] Service de Néonatalogie et Réanimation Néonatale de la Croix-rousse, Hôpitaux Civils de Lyon, Lyon, France
[f] Service de Néonatalogie et Réanimation Néonatale, Hôpital Femme-Mère-Enfant, Bron, France
[g] EA 4129, Université Claude Bernard Lyon 1, Villeurbanne, France

Keywords:

A B S T R A C T

Objectives: To observe hyperechoic nodular or punctate white matter lesions (HNPL) in a population of preterm infants using routine cranial ultrasound (cUS), to describe the characteristics of HNPL, and to compare them with punctate white matter lesions (PWML) detected in magnetic resonance imaging (MRI).
Design: Retrospective observational single-center cohort study.
Setting: Level 2B neonatal unit in France.
Patients: 307 infants born <33 weeks gestation undergoing routine cUS with a total of 961 cUS performed.
Main outcome measures: Description of lesions (HNPL/PWML): presence or absence, number, size, location, and structural distribution.
Results: Among the 307 included infants, 63 (20.5%) had at least one cerebral lesion, with 453 HNPL for 63 infants. HNPL were numerous (more than three in 66.6% of cases), primarily grouped in clusters (76.2%), located near the lateral ventricles (96.8%), and measuring more than 2 mm (79%). HNPL were diagnosed on day 29 on average and persisted until term. Overall, 43 MRI were performed in 307 infants, on average 18.9 days after last cUS, in 21 of those the indication was presence of HPNL on cUS. Of these 21 MRI, 14/21 presented 118 PWML compared to 173 HNPL on cUS. In the remaining MRI (7/21), no PWML were detected compared to 47 HNPL on cUS.
Conclusions: In our population of 307 preterm infants, cUS allowed the diagnosis of HNPL, with a large similarity to PWML in MRI and a better sensitivity. But in the absence of data on inter-observer variability, we cannot exclude overdiagnosis of HNPL.

1. Introduction

Infants born prematurely are at risk for neurodevelopmental impairments, often related to white matter (WM) injuries. Over the last 30 years, the incidence of severe WM lesions has decreased significantly [1], whereas the incidence of neurodevelopmental impairments remains high and can even exceed 50% in infants born at 24–26 weeks gestation [2]. Magnetic resonance imaging (MRI) of the neonatal brain has contributed to identifying non-cystic WM lesions, which are more localized and subtler than the larger cystic lesions seen in more severe WM injury, appearing as punctate high signal intensity lesions on T1-weighted imaging. These punctate white matter lesions (PWML) are identified in 18%–35% of preterm infants born <33 weeks gestation [3]. Their involvement in neurodevelopmental abnormalities was recently confirmed [4–8], making their diagnosis an important objective for MRI. However, there are several limitations in this respect. The indications for MRI vary depending on the neonatal units and the often-limited availability of this specialized imaging technique. While a few neonatal units include MRI in their routine care of infants born <32 weeks gestation [6, 9], the majority only use it for infants born <28 weeks gestation or in the

* Corresponding author.

case of significant abnormalities detected on cranial ultrasound (cUS) [10,11], representing less than 35% of preterm infants born <32 weeks gestation based on the Epipage2 cohort [12]. This heterogeneity of practices means that the screening for PWML is quite random. Finally, PWML tend to fade over time and 1/3 of cases may have disappeared at term [10,13–15].

Given its major advantages, including the low cost, the sequential use of ultrasound in the entire population of preterm infants could facilitate the broader screening for PWML. However, PWML, which are suspected on ultrasound at best in less than 50% of cases [16], are mostly undiagnosed on cUS [4] and have not been systematically described in the literature.

The objective of this study was to observe hyperechoic nodular or punctate white matter lesions (HNPL) in a population of preterm infants using routine cUS, to describe HNPL characteristics, and then to compare them with the PWML described in MRI.

2. Patients and methods

2.1. Patients

This is a monocentric retrospective study. Between January 2013 and December 2016, 332 consecutive preterm infants born <33 weeks gestation were hospitalized in the neonatal unit (maternity level 2B), either at birth or after discharge from the NICU.

A total of 25 infants were excluded: two deaths in the first 24 h, seven intensive care transfers, five congenital malformations, three infants who did not undergo cUS, one parent refusal and 7 infants which parents were unreachable (Fig. 1). Consequently, 307 families provided consent in line with the French and European legislation. The study was approved by the Ethics Committee CPP SUD-EST VI (2022/CE47).

An initial retrospective review of all cUS examinations performed in the 307 remaining infants, classified the infants into two groups based on the presence of nodular WM lesions: cUSgroup1 (HNPL+) with at least one HNPL and cUSgroup2 (HNPL-) without HNPL.

A second review of the cUSgroup1 described the characteristics of the lesions. The retrospective HNPL + classification was then compared with the classification made during the neonatal stay.

After these two retrospective reviews, each infant's medical record was reviewed for MRI analysis. In cUSgroup1, 21 infants had MRI images (MRIgroup1). In cUSgroup2, 22 infants with MRI images were identified (MRIgroup2). These images were reviewed by two independent neuroradiologists.

2.2. Cranial UltraSound (cUS)

2.2.1. Examinations

cUS were performed, by 5 neonatologists, every 2 weeks, upon admission to the unit, until discharge, and at term using a Siemens Acuson 2000 ultrasound system with a 10V4 neonatal vector probe, routinely supplemented by a Multi-D matrix 9L4 linear probe and dynamic sequences (DS) in coronal sections (about 300 images). The images and DS were stored on an external hard drive and viewed using a Dicom viewer (RadiAnt Dicom viewer, Medixant). cUS were repeated on average 2.19 times per child.

2.2.2. Assessment of brain lesions on cUS

The neonatologist, who reviewed retrospectively all the cUS, has 25 years of experience in the field consolidated by exchanges with regional neuropediatricians. Interobserver variability studies were not performed due to a lack of regional expert.

The following criteria were used to define HNPL: hyperechoic lesions with a round or oval shape >2 mm or punctate lesions measuring 1–2 mm, at least or nearly as echoic as the choroid plexuses [17], located in deep or periventricular WM, halfway between the lateral ventricles (LV) and the depths of the cortical sulci or in the axis of the convolutions (Supplemental Fig. 1). These lesions did not show any physiological hyperechoic characteristics [18,19].

The linear distribution of the HNPL was defined as nodular lesions aligned in parallel to the axis of LV frontal horns (Supplemental Fig. 1), whereas the cluster appearance of HNPL was defined as single or multiple lesions, grouped together in clusters without alignment.

The diagnosis "HNPL+" was retained if at least one lesion was detected by at least one cUS. In the absence of specific training in HNPL diagnosis, either in-house or by external reviewers, initial diagnosis and review could only be performed by the principal author. So, cross-reading was not possible. The lead author performed a total of 506/961 cUS (1–5 cUS per child, in 80.6% of children).

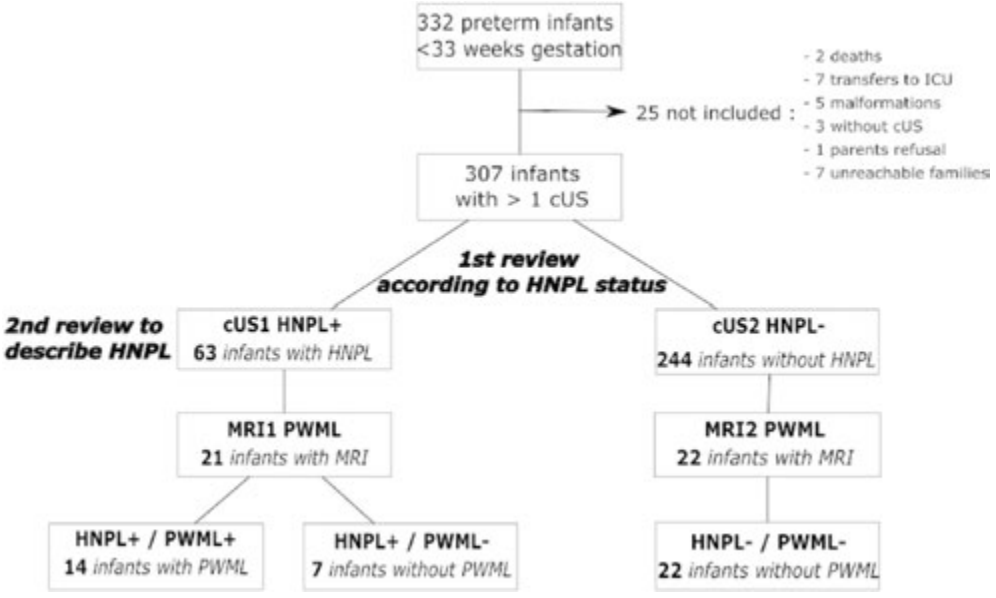

Fig. 1. *Flow diagram of the study participants*
Abbreviation: cUS: cranial UltraSound; HNPL: Hyperechoic Nodular or Punctate white matter Lesions; MRI: Magnetic Resonance Imaging; PWML: Punctate White Matter lesions.

2.2.3. Additional cUS methodology

For the 21 infants who presented the most HNPL (14 with more than ten HNPL and 7 with between four and ten HNPL), the 2D ultrasound images were transformed into 3D cUS from DS obtained by a free-hand ultrasound sweep around an axis represented by the coronal suture [20–23]. For these 21 infants, HNPL were manually segmented on a touch screen computer (Surface Studio 28″, open-access software mitk) and arranged in a common reference frame [24]. This 3D reconstruction method allowed cUS and MRI images to be compared in strictly similar plan, especially in the axial plane.

2.3. MRI

2.3.1. MRI examination

Because this is a retrospective study, MRI indications were in line with the current clinical practice of the unit. Brain MRI was performed at term in the general radiology department of the hospital, either because of suspected PWML on cUS (on average 12 HNPL per child) or routinely in infants born <28 weeks gestation or in those presenting significant abnormalities other than HNPL on cUS, such as significant white matter lesions (cPVL, PHI) or primary ventricular dilatation. cUS and MRI were not done on the same day, for logistical reasons. The average time from last cUS to MRI was 18.9 days ± 24.3.

2.3.2. Brain MRI analysis

MRI images were interpreted by a radiologist trained in neonatal brain injury. The presence of PWML as well as their number, location, and type (linear, cluster, or mixed) were detailed. Two external expert pediatric neuroradiologists, who knew the ultrasound diagnosis, conducted their unblinded review together. No interrater variability study was performed. The characteristics of lesions were compared with the HNPL observed on cUS.

2.3.3. MRI protocol

The examinations were performed with Achieva system 1,5T (Philips Healthcare, Best, the Netherlands), a 16 channels adult antenna, without sedation, with swaddling in a Cocoonababy foam cocoon (Redcastle), using a 3 M earplug and a Philips headset, after a bottle.

The routine protocol included: 3DT1-weighted,TR 7,8 ms,TE 3,6 ms, slice thickness 1,1 mm, Gap 0 mm,T1-weighted SE axial, TR 696 ms,TE 12 ms,slice thickness 3,5 mm, gap 0,5 à 1 mm, T2-weighted axial, TR 4500 ms, TE 200 ms, slice thickness 4,5 mm, gap 1 mm, T2*-weighted GRE, TR 638 ms, TE 23 ms,slice thickness 5,3 mm, gap 1 mm, Diffusion HR sense, TR 4206 ms, TE 75 ms, slice thickness 4 mm, gap 1 mm.

2.4. Data collection and statistical analysis

Statistical analyses were performed using IBM SPSS Statistics version 20.0 (IBM SPSS Inc., Chicago, IL, USA). Quantitative variables are presented as means with standard deviations (SD) and 95% confidence intervals (CI) or as medians with interquartile ranges. Qualitative variables are presented as numbers and percentages with 95% CI. The relation between two qualitative variables (comparison of percentages) was evaluated using Pearson's chi-square test or Fisher's test exact where applicable. The relation between quantitative and qualitative variables with two modalities was evaluated using Student's *t*-test for independent samples. The level of significance was fixed at $p < 0.05$.

3. Results

3.1. Patient characteristics

The study included 307 infants (162 boys and 145 girls) with a mean gestational age of 30.2 weeks (±1.88) at delivery and a mean birth weight of 1430g (±374). In total, 104 infants (33.9%) were twins, and 220 were born by cesarian section (71.7%) (Table 1). The first review of

Table 1
Comparison of maternal and neonatal clinical characteristics of the two groups with and without HNPL on cUS. HNPL: hyperechoic, nodular or punctate white matter lesions; SD: standard deviation; *Ophthalmoscopy performed in 70% of infants; White matter lesions (periventricular hemorrhagic infarction, kystic and non kystic leukomalacia).

	TOTAL n = 307	HNPL – n = 244	HNPL + n = 63	p-value
Antenatal complications				
Intrauterine growth restriction (IUGR) – n (%)	21 (6.8%)	16 (6.6%)	5 (7.9%)	0.699
Preeclampsia – n (%)	***75 (24.4%)***	***66 (27.0%)***	***9 (14.3%)***	***0.036****
Pre-labor rupture of membrane (PRM) – n (%)	111 (36.2%)	85 (34.8%)	26 (41.3%)	0.343
Chorioamnionitis – n (%)	40 (13.0%)	30 (12.3%)	10 (15.9%)	0.452
Mode of delivery				
Induction – n (%)	159 (51.8%)	132 (54.1%)	27 (42.9%)	0.111
C-section – n (%)	220 (71.7%)	176 (72.1%)	44 (69.8%)	0.719
Antenatal treatment or during labor				
Antenatal corticosteroid therapy – n (%)	***221 (72.0%)***	***182 (74.6%)***	***39 (61.9%)***	***0.046****
Sulfate magnesium++ – n (%)	***72 (23.5%)***	***50 (20.5%)***	***22 (34.9%)***	***0.016****
Infant characteristics				
Gestational age (weeks) – mean (SD)	30.2 (1.88)	30.2 (1.92)	30.3 (1.74)	0.684
Birth weight (g) – mean (SD)	1430 (374)	1419 (369)	1476 (390)	0.267
Sex ratio M/F – n (%)	162/145	129/115	33/30	0.945
Twin zygosity – n (%)	104 (33.9%)	83 (34.0%)	21 (33.3%)	0.919
Apgar score – mean (SD)	8.78 (1.67)	8.8 (1.70)	8.73 (1.57)	0.776
Arterial pH – mean (SD)	7.26 (0.12)	7.26 (0.12)	7.26 (0.13)	0.845
Infant treatments				
Intubation – n (%)	19 (6.2%)	16 (6.6%)	3 (4.8%)	0.774
Mechanical ventilation – n (%)	102 (33.2%)	75 (30.7%)	27 (42.9%)	0.069
Surfactant treatment – n (%)	***115 (37.5%)***	***84 (34.4%)***	***31 (49.2%)***	***0.031****
Days of oxygen ventilation – mean (SD)	11.36 (58.63)	12.13 (63.23)	7.2 (19.38)	0.644
Catecholamine treatment – n (%)	11 (3.6%)	8 (3.3%)	3 (4.8%)	0.702
Total parenteral nutrition – n (%)	7 (2.3%)	6 (2.5%)	1 (1.6%)	1
Infant complications				
Early onset neonatal sepsis – n (%)	5 (1.6%)	4 (1.6%)	1 (1.6%)	1
Sepsis – n (%)	37 (12.1%)	27 (11.1%)	10 (15.9%)	0.296
Infantile respiratory distress syndrome - n (%)	***125 (40.7%)***	***92 (37.7%)***	***33 (52.4%)***	***0.035****
Bronchopulmonary dysplasia – n (%)	18 (5.9%)	13 (5.3%)	5 (7.9%)	0.432
Necrotizing enterocolitis – n (%)	12 (3.9%)	10 (4.1%)	2 (3.2%)	1
Patent ductus arteriosus – n (%)	25 (8.1%)	17 (7.0%)	8 (12.7%)	0.306
Retinopathy of prematurity – n (%)*	47 (21.9%)	40 (23.3%)	7 (16.3%)	0.413
Pathological neurological exploration – n (%)	7 (2.3%)	5(2.0%)	2 (3.2%)	0.637
Intraventricular hemorrhage grade 2–3 – n (%)	19 (6.2%)	13 (5.3%)	6 (9.5%)	0.218
White matter lesions – n (%)	***12 (3.9%)***	***6 (2.5%)***	***6 (9.5%)***	***0.010****

all cUS examination identified 63 infants with at least one HNPL and 244 infants without any HNPL (Fig. 1).

3.2. Between-group differences

The two populations with and without HNPL were comparable for most descriptive items. Nevertheless, the presence of HNPL was significantly associated with respiratory distress syndrome ($p = 0.035$), surfactant treatment ($p = 0.031$), WM lesions (*periventricular hemorrhagic infarction, cystic or noncystic leukomalacia* ($p = 0.010$), and magnesium sulfate administration ($p = 0.016$), while it was inversely correlated with preeclampsia ($p = 0.036$) and antenatal corticosteroid therapy ($p = 0.046$) (Table 1).

3.3. Ultrasound examinations

A total of 961 cUS were performed in 307 included infants. HNPL were identified in 63 infants (20.5%), with an increasing prevalence over the 4 years of the study (Table 2) due to a probable learning curve. The presence of HNPL was confirmed on several consecutive cUS. cUS were repeated on average 2.19 times per child.

These 63 infants had a total of 453 HNPL. The lesion load per infant, their size, location, and type are summarized in Table 3. Nodular lesions were primarily isolated or grouped in clusters (76.2%) and located in the central WM region (82.5%) with regard to the LV. Almost half of infants (44.4%) had four to ten lesions, often very large and measuring 2–5 mm (67.1%) (Table 3).

On average, the diagnosis was made on day 29, corresponding to a corrected age of 34 weeks + 6. The lesions persisted until the end of the neonatal stay and were still observable at term (38 weeks + 1). In 24% of cases, we observed an attenuation of echogenicity of the lesions, but never their disappearance.

Punctate lesions were isoechoic to the choroid plexuses in 92% of cases. Their echogenicity increased during the stay in 3.4% of cases, remained stable in the majority of cases (72%), or regressed without completely disappearing in 24.6% of infants (data not shown).

The 3D lesion map showed the grouping of HNPL in the central WM region, alongside and at a distance from the LV frontal horns (coronal view, Fig. 2).

3.4. MRI

MRI was performed in 43 out of 307 infants (14%). In cUSgroup1, 21 MRI (MRIgroup1) were conducted at a PMA of 39 weeks + 5 (range: 35 weeks + 3–50 weeks). Fourteen out of these 21 MRI (HNPL+/PWML+) identified 118 PWML: five cases were linear, seven were clustered, and two were mixed (Table 4). The remaining seven MRI (HNPL+/PWML-) did not show any PWML. A post-IVH grade 3 triventricular dilatation and a perforator stroke were identified.

T2*-weighted sequences identified three cases of periventricular hemosiderin deposition (HIV1), twice associated with PWML. In one infant, a small isolated hemorrhage was detected under the frontal cortex. No PWML were associated with a distinct hyposignal compatible with hemorrhage. All MRI lesions were also detected by cUS.

Table 2
Concordance between the initial HPNL + diagnosis by cUS during the neonatal stay (initial diagnosis), and the final diagnosis retained for the study after the first screening. HNPL: hyperechoic, nodular, or punctate white matter lesion.

Years	2013	2014	2015	2016
Preterm infants gestational age < 33 weeks	74	98	65	70
Number of HNPL+ (%)	5 (6.8%)	13 (13.3%)	20 (30.8%)	25 (35.7%)
Concordance initial/final diagnosis (%)	5/5 (100%)	7/13 (53.8%)	14/20 (70%)	19/25 (76%)

Table 3
Characteristics of hyperechoic, nodular, or punctate white matter lesions. Overall: diffuse localized lesions, i.e., in at least two of the mentioned regions.

	Number - n (%)	Total - n
Appearance (n = infants)		
Linear	9 (14.3)	63
Cluster	48 (76.2)	
Mixed	6 (9.7)	
Location (n = infants)		
Anterior	0 (0)	63
Central	52 (82.5)	
Posterior	2 (3,2)	
Overall	9 (14.3)	
Lesion Load (n = infants)		
1-3	21 (33.3)	63
4-10	28 (44.4)	
>10	14 (22.2)	
Size (n = lesions)		
<2 mm	96 (21.2)	453
2 < … < 5 mm	304 (67.1)	
>5 mm	53 (11.7)	

In cUSgroup2, 22 MRI (MRI group 2) were performed at a PMA of 41 weeks + 5 (range: 34 weeks + 2–55 weeks + 2), detecting four post-IVH grade 2–3 with dilatation, one perforator ischemic stroke, one superior longitudinal sinus thrombosis, and two cystic WM lesions (one cystic periventricular leukomalacia with periventricular hemorrhagic infarction and one unilateral periventricular hemorrhagic infarction). In this group, only one child showed one isolated low-intensity lesion with no other associated white matter lesion. Overall, 14 MRI were normal. All MRI lesions were also detected by cUS.

3.5. Comparison between cUS and MRI

In the HNPL+/PWML + subgroup, cUS identified 173 HNPL (four linear, five cluster, and four mixed), while MRI only detected 118 PWML (five linear, seven cluster, and two mixed) (Table 4).

In the HNPL+/PWML-subgroup, cUS identified 47 HNPL (one linear and six cluster), while no PWML were detected with MRI (Table 4).

In terms of morphology, the HNPL can be similar to the PWML detected in MRI in terms of their location, size, and shape. The lesions with a linear pattern were parallel to the LV frontal horns in 4 out of 5 cases (Fig. 3).

For the 3D reconstruction, we chose the 3D US slices most similar to the MRI slices and observed many similarities between HNPL and PWML, in the axial and coronal planes which are usually inaccessible on cUS. These similarities were particularly visible in five infants from the HNPL+/PWML + subgroup (Fig. 4) in terms of their location (AA'/BB' and KK'/LL'), size, and shape (EE'/FF' and II'/JJ), notably the comma-shaped appearance of one PWML in the left semioval centrum (EE'/FF').

4. Discussion

The aim of this study was to retrospectively analyze HNPL identified on cUS in a population of preterm infants and to compare them with PWML detected in MRI.

This investigation allowed us to observe that several HNPL characteristics such as the shape, size, or location of the hyperechoic lesions can be superposed on the WM hypersignals in T1-weighted MRI. In addition, we showed some hyperechoic nodules were aligned with periventricular WM along the LV anterior horns, observed in the same location on both parasagittal cUS and sagittal T1-weighted MRI slices.

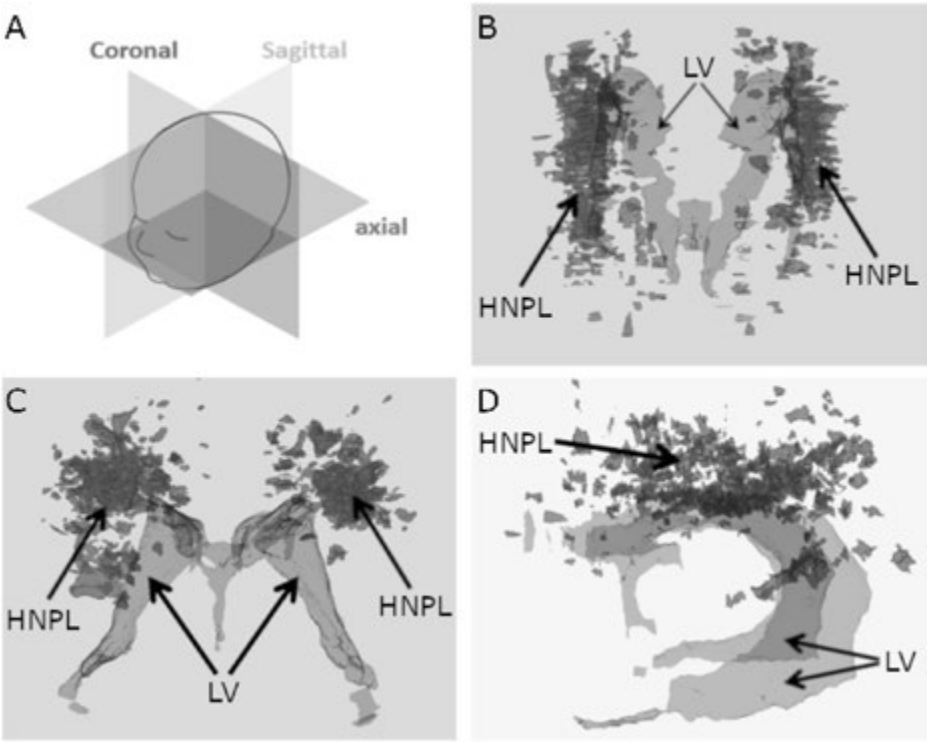

Fig. 2. *3D lesion map*
Distribution map in the 3 spatial planes (**B**: Axial plan, **C**: Coronal plan, **D**: Sagittal plan) of HNPL (in dark grey) segmented manually on cUS 3D (obtained after reconstruction from images of 2D dynamic sequences) in 21 of the 63 children of the HNPL + cohort. Abbreviation: LV: Lateral Ventricles; cUS: cranial UltraSound; HNPL: Hyperechoic Nodular or Punctate white matter Lesions (in dark grey).

Table 4
Comparison of cUS and MRI imaging in 21 HNPL + children who underwent an MRI (MRI group 1): number of children and lesions according to the lesion shape. HNPL: hyperechoic, nodular, or punctate white matter lesion. PWML: Punctate White Matter Lesion.

Lesion shape	Infants (n)				Lesions (n)			
	HNPL+/PWML+		HNPL+/PWML-		HNPL+/PWML+		HNPL+/PWML-	
	HNPL	*PWML*	*HNPL*	*PWML*	*HNPL*	*PWML*	*HNPL*	*PWML*
Linear	4	5	1	0	80	44	10	0
Cluster	6	7	6	0	27	38	37	0
Mixed	4	2	0	0	66	36	0	0
Total	14	14	7	0	173	118	47	0

This linear pattern has already been described in the MRI-literature [10,25,26].

This study confirmed a mean incidence of HNPL of around 20%, which is described in the literature for PWML [27,28]. Even if the existing MRI-data are heterogeneous [4,13,29], several risk factors for PWML were identified in this study on HNPL: hypertension [29], no steroid therapy, immediate intubation [13,29], mechanical ventilation [4,15]. Regarding neuroprotection with magnesium sulfate, the paradoxically higher prevalence of HNPL (29% vs. 17%, $p < 0.03$) could be explained by a lower gestational age (29.24 S A vs. 30.52, $p < 0.001$) and a more frequent association with sepsis (19% vs. 10%, $p < 0.028$) or bronchopulmonary dysplasia (11% vs. 4%, $p < 0.043$). In addition, during the study period, the indication for neuroprotection with magnesium sulfate was not yet protocolized and was left to the responsibility of each practitioner, which probably explains the lower gestational age.

Aside from the similarities between HNPL and PWML, there are several differences. In our study, HNPL persisted until term even if attenuated in 24.6% of cases, whereas in the literature, PWML regressed and disappeared in more than a third of cases [10,13,15]. In children undergoing MRI due to the presence HNPL on cUS, only two-thirds presented PWML and in smaller quantities. In this study, almost twice as many lesions were identified on cUS than in MRI.

In the literature, PWML described in MRI over the past 20 years are rarely suspected on ultrasound, at best in less than 50% of cases [16]. They are mostly undiagnosed on cUS [4] and have not been systematically described. A recent US classification of WM abnormalities was proposed by the eurUS.brain group, including hyperechoic masses labelled as punctate gliosis, hyperechoic gliotic nodules, or clusters of multiple hyperechoic dots [19].

High-end ultrasound and high-resolution linear probes with large angles of insonation can more accurately describe WM abnormalities [19,30]. In our study, the routine use of a Multi-D matrix 1.5D linear probe with a large trapezoidal field resulted in the better detection of punctate lesions on cUS compared to MRI. This unusual finding can be partly explained by the better contrast resolution of the linear pseudo-matrix probes, thanks to the layout of piezoelectric crystals in three parallel rows used in this study [31].

In our study, cUS was more sensitive than MRI, which is surprising given the difficulties associated with the cUS diagnosis of PWML. Nevertheless, the detection of PWML in MRI depends on the type and

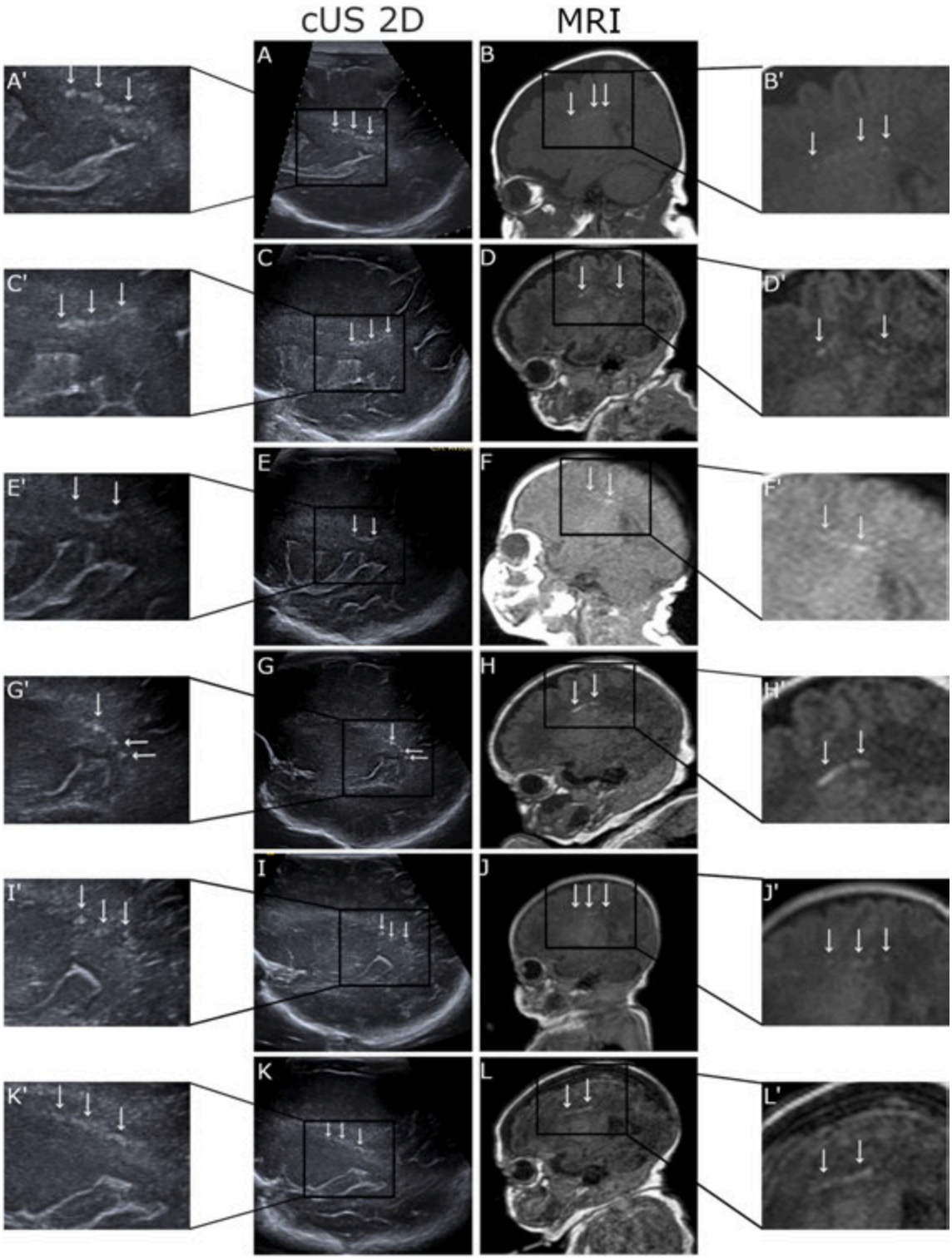

Fig. 3. *Comparison of sagittal US and MRI*
Comparison of sagittal US (**A**, **C**, **E**, **G**, **I** and **K**) and MRI (**B**, **D**, **F**, **H**, **J** and **L**) slices, in a close plane, taken close to term, on the same day, in 6 children with a linear form of lesions. Arrows showed HNPL or PWML on cUS 2D or MRI images, respectively. Abbreviation: cUS: cranial UltraSound; HNPL: Hyperechoic Nodular or Punctate white matter Lesions; MRI: Magnetic Resonance Imaging; PWML: Punctate White Matter lesions.

spatial resolution of the sequences [32]. Ideally, the voxels should be less than 1 mm^3 on the 3D sequences [3], as in our study (1.1x1.1 × 1.1 mm), even if the magnetic field strength was only 1.5T. The pixels on cUS (0.168 × 0.168 mm with the 9L4 probe) were much smaller than in MRI, which could partly explain the better spatial resolution of cUS in this study, and indirectly, the persistence of HNPL during the neonatal stay.

The high precision of new linear probes, like the one we've used, has allowed us to observe these HNPL. It has also changed our practice, allowing us to get much finer images of the white matter echo structure, especially regarding arterial vascularization, which must be differentiated from punctate lesions. In complex cases, reviewing the dynamic

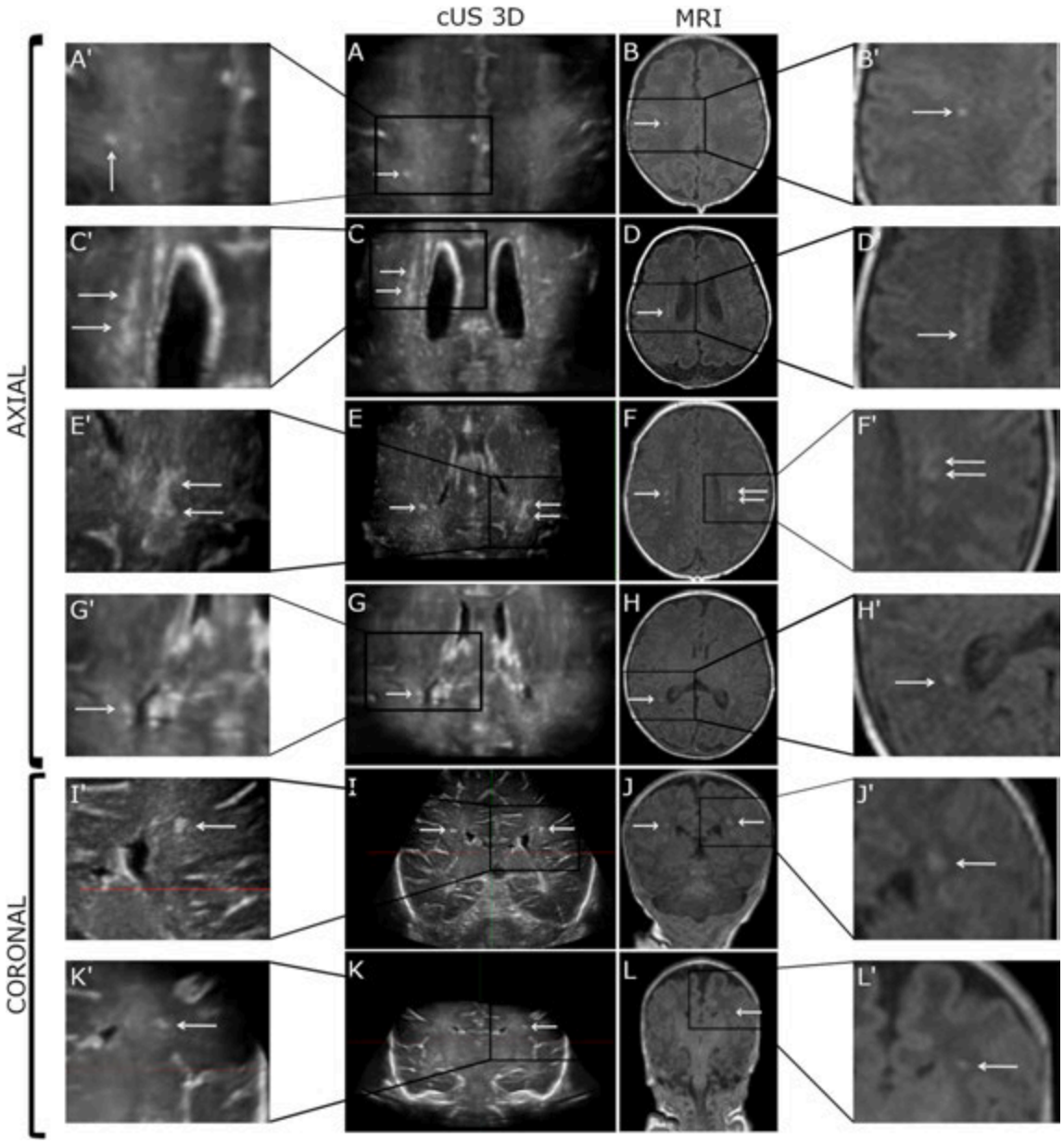

Fig. 4. *Comparison of 3D cUS and T1 MRI axial and coronal sections*
Comparison in an almost identical plane of the 3D cUS (**A**, **C**, **E**, **G**, **I** and **K**) and T1 MRI sections (**B**, **D**, **F**, **H**, **J**, and **L**) taken close to the term, on the same day, in 6 children with a linear or mixed form of HNPL (cUS 3D sections made by the research laboratory Creatis- Insa, Université Lyon1, after 3D reconstruction of 2D dynamic sequences obtained by hand-free scanning). The axial (**A**, **B**, **C**, **D**, **E**, **F**, **G** and **H**) and coronal (**I**, **J**, **K** and **L**) sections were shown. **A′**, **B′**, **C′**, **D′**, **E′**, **F′**, **G′**, **H′**, **I′**, **J′**, **K′** and **L′** images were the enlargement of **A**, **B**, **C**, **D**, **E**, **F**, **G**, **H**, **I**, **J**, **K** and **L** images, respectively. Arrows showed HNPL or PWML on cUS 3D or MRI images respectively. Abbreviation: cUS: cranial UltraSound; HNPL: Hyperechoic Nodular or Punctate white matter Lesions; MRI: Magnetic Resonance Imaging; PWML: Punctate White Matter lesions.

sequences, image by image, to obtain a volumetric image of the lesion, has often been a key to our conclusions.

2D cUS did not accurately localize the lesions in the coronal and sagittal slices or even produce axial slices. 3D ultrasound has long since proven its value in pediatrics, particularly on cUS [33,34], for which its diagnostic performance is equivalent to 2D cUS for the majority of abnormalities with a considerable saving of time [35,36].

The use of a 3D matrix of images obtained from the coronal DS allowed us to compare for some infants the location of the lesions, their size, and shape in the three radiological planes, particularly the axial plane, which is completely inaccessible on cUS. In these cases, HNPL were very similar to PWML identified in MRI.

This study presents several others limitations, particularly because of its retrospective and monocentric nature. Due to the lack of expert reviewer, we were not able to study the interobserver variability. MRI was performed on a 1.5T system and a 3T system would probably have detected more PWML. As both examinations were performed according to standard practice, cUS and MRI were not performed on the same day. There was a time interval between last cUS and MRI. This may have played a role in the underestimation of PWML on MRI. Moreover, the diagnosis of HNPL followed a learning curve during the study, and HNPL were only exhaustively verified in the last 2 years following the systematic use of DS.

Even in favorable examination conditions, the diagnosis of punctate lesions on cUS remains challenging, especially for small lesions, peripheral lesions, or slightly echogenic lesions. Several diagnoses of

punctate lesions were missing and were only made during the interpretation phase, notably at the start of the study. Conversely, it is possible to overestimate the diagnosis of HNPL, especially in cases of misinterpretation of vascular images or calcifications. In addition, their diagnosis required the use of high-end cUS, which does not always meet the versatility and mobility requirements for ultrasounds in neonatal units.

In addition to the difficulty in diagnosing these subtle WM lesions, interobserver variability is another important limitation on cUS [37–40].

This highlights the value of computer-assisted technology for the diagnosis and image processing [19] and artificial intelligence algorithms for the automatic detection of the lesions [22–24]. A prospective study comparing 2D/3D cUS and MRI could confirm the similarity between HNPL and PWML and also train artificial intelligence algorithms to improve the cUS identification of PWML in routine practice.

Another prospective study is needed to confirm the improved sensitivity of ultrasound observed in this study. In practice, this diagnosis remains difficult, requiring a top-of-the-range cUS equipped with a linear probe and an adaptation of the examination protocol. This first description of PWML on cUS highlights the possibility of diagnosing preterm infants who cannot benefit from MRI and underlines the importance of developing diagnostic assistance technology adapted to ultrasound.

5. Conclusion

The hyperechoic nodular WM lesions presented in this retrospective study show a great similarity with the PWML described in MRI in the literature. To our knowledge, HNPL have not been systematically described. Technological advances in imaging could facilitate the US diagnosis of PWML, which remains challenging, particularly in the large population of preterm infants who do not benefit from MRI.

Funding sources

This work was partially performed within the framework of the LABEX PRIMES (ANR-11-LABX-0063) and supported by the LABEX CELYA (ANR-10-LABX-0060) of Université de Lyon, within the program “Investissements d’Avenir" (ANR-11-IDEX-0007) operated by the French National Research Agency (ANR).

Ethical statement

The study was approved by the French Ethics Committee CPP SUD-EST VI (2022/CE47).

Declaration of competing interest

All authors declare no conflict of interest.

Acknowledgment

The authors would like to thank all the participating children and their parents.

Appendix A. Supplementary data

Supplementary data to this article can be found online at https://doi.org/10.1016/j.ejpn.2024.02.014.

References

[1] I.C. van Haastert, F. Groenendaal, C.S.P.M. Uiterwaal, et al., Decreasing incidence and severity of cerebral palsy in prematurely born children, J. Pediatr. 159 (2011) 86–91.e1.

[2] V. Pierrat, L. Marchand-Martin, S. Marret, et al., Neurodevelopmental outcomes at age 5 among children born preterm: EPIPAGE-2 cohort study, BMJ 373 (2021) n741.

[3] A.L.A. Nguyen, Y. Ding, S. Suffren, et al., The brain’s kryptonite: overview of punctate white matter lesions in neonates, Int J Dev Neurosci Off J Int Soc Dev Neurosci 77 (2019) 77–88.

[4] N. Tusor, M.J. Benders, S.J. Counsell, et al., Punctate white matter lesions associated with altered brain development and adverse motor outcome in preterm infants, Sci. Rep. 7 (2017) 13250.

[5] F.T. de Bruïne, A.A. van den Berg-Huysmans, L.M. Leijser, et al., Clinical implications of MR imaging findings in the white matter in very preterm infants: a 2-year follow-up study, Radiology 261 (2011) 899–906.

[6] T.Y. Jeon, J.H. Kim, S.-Y. Yoo, et al., Neurodevelopmental outcomes in preterm infants: comparison of infants with and without diffuse excessive high signal intensity on MR images at near-term-equivalent age, Radiology 263 (2012) 518–526.

[7] C. Arberet, M. Proisy, J.L. Fausser, et al., Isolated neonatal MRI punctate white matter lesions in very preterm neonates and quality of life at school age, J. Neonatal Perinat. Med. 10 (2017) 257–266.

[8] C.A.M. de Bruijn, S. Di Michele, M.L. Tataranno, et al., Neurodevelopmental consequences of preterm punctate white matter lesions: a systematic review, Pediatr. Res. (9 September 2022), https://doi.org/10.1038/s41390-022-02232-3. Published Online First.

[9] V. Neubauer, T. Djurdjevic, E. Griesmaier, et al., Routine magnetic resonance imaging at term-equivalent age detects brain injury in 25% of a contemporary cohort of very preterm infants, PLoS One 12 (2017) e0169442.

[10] K.J. Kersbergen, M.J.N.L. Benders, F. Groenendaal, et al., Different patterns of punctate white matter lesions in serially scanned preterm infants, PLoS One 9 (2014) e108904.

[11] M. Guillot, V. Chau, B. Lemyre, Routine imaging of the preterm neonatal brain, Paediatr. Child Health 25 (2020) 249–262.

[12] P.-Y. Ancel, F. Goffinet, EPIPAGE-2 Writing Group, Survival and morbidity of preterm children born at 22 through 34 weeks’ gestation in France in 2011: results of the EPIPAGE-2 cohort study, JAMA Pediatr. 169 (2015) 230–238.

[13] N. Wagenaar, V. Chau, F. Groenendaal, et al., Clinical risk factors for punctate white matter lesions on early magnetic resonance imaging in preterm newborns, J. Pediatr. 182 (2017) 34–40.e1.

[14] L.E. Dyet, N. Kennea, S.J. Counsell, et al., Natural history of brain lesions in extremely preterm infants studied with serial magnetic resonance imaging from birth and neurodevelopmental assessment, Pediatrics 118 (2006) 536–548.

[15] M.A. Rutherford, V. Supramaniam, A. Ederies, et al., Magnetic resonance imaging of white matter diseases of prematurity, Neuroradiology 52 (2010) 505–521.

[16] G. Ciambra, S. Arachi, C. Protano, et al., Accuracy of transcranial ultrasound in the detection of mild white matter lesions in newborns, NeuroRadiol. J. 26 (2013) 284–289.

[17] G. van Wezel-Meijler, M.S. van der Knaap, L.T. Sie, et al., Magnetic resonance imaging of the brain in premature infants during the neonatal period. Normal phenomena and reflection of mild ultrasound abnormalities, Neuropediatrics 29 (1998) 89–96.

[18] L.M. Leijser, L. Srinivasan, M.A. Rutherford, et al., Frequently encountered cranial ultrasound features in the white matter of preterm infants: correlation with MRI, Eur J Paediatr Neurol EJPN Off J Eur Paediatr Neurol Soc 13 (2009) 317–326.

[19] T. Agut, A. Alarcon, F. Cabañas, et al., Preterm white matter injury: ultrasound diagnosis and classification, Pediatr. Res. 87 (2020) 37–49.

[20] M. Martin, B. Sciolla, M. Sdika, et al., Automatic segmentation and location learning of neonatal cerebral ventricles in 3D ultrasound data combining CNN and CPPN, Comput. Biol. Med. 131 (2021) 104268.

[21] M. Martin, B. Sciolla, M. Sdika, et al., Automatic Segmentation of the Cerebral Ventricle in Neonates Using Deep Learning with 3D Reconstructed Freehand Ultrasound Imaging, vols. 1–4, 2018, https://doi.org/10.1109/ULTSYM.2018.8580214.

[22] F. Estermann, V. Kaftandjian, P. Guy, et al., PWML detection in 3D cranial ultrasound volumes using over-segmentation and multimodal classification with deep learning, in: 2023 IEEE 20th International Symposium on Biomedical Imaging (ISBI), IEEE, 2023, pp. 1–5, https://doi.org/10.1109/ISBI53787.2023.10230607. Cartagena, Colombia.

[23] F. Estermann, V. Kaftandjian, P. Guy, et al., Vision transformer and multi-view classification for lesion detection in 3D cranial ultrasound, IEEE Ultrasonics symposium (2023) p1–p4.

[24] P. Erbacher, C. Lartizien, M. Martin, et al., Priority U-net: detection of punctuate white matter lesions in preterm neonate in 3D cranial ultrasonography priority u-Net for detection of pwml in preterm 3d cranial ultrasonography, Montreal, Canada, Medical Imaging with Deep Learning (MIDL) (2020), 205–16, https://hal.archives-ouvertes.fr/hal-02995667. (Accessed 1 April 2022).

[25] L.G. Cornette, S.F. Tanner, L.A. Ramenghi, et al., Magnetic resonance imaging of the infant brain: anatomical characteristics and clinical significance of punctate lesions, Arch. Dis. Child. Fetal Neonatal Ed. 86 (2002) F171–F177.

[26] C. Raybaud, T. Ahmad, N. Rastegar, et al., The premature brain: developmental and lesional anatomy, Neuroradiology 55 (Suppl 2) (2013) 23–40.

[27] L.S. de Vries, M.J.N.L. Benders, F. Groenendaal, Progress in neonatal neurology with a focus on neuroimaging in the preterm infant, Neuropediatrics 46 (2015) 234–241.

[28] M.J.N.L. Benders, K.J. Kersbergen, L.S. de Vries, Neuroimaging of white matter injury, intraventricular and cerebellar hemorrhage, Clin. Perinatol. 41 (2014) 69–82.

[29] A. Parodi, M. Malova, V. Cardiello, et al., Punctate white matter lesions of preterm infants: risk factor analysis, Eur J Paediatr Neurol EJPN Off J Eur Paediatr Neurol Soc 23 (2019) 733–739.
[30] G. van Wezel-Meijler, S.J. Steggerda, L.M. Leijser, Cranial ultrasonography in neonates: role and limitations, Semin. Perinatol. 34 (2010) 28–38.
[31] D.G. Wildes, R.Y. Chiao, C.M.W. Daft, et al., Elevation performance of 1.25D and 1.5D transducer arrays, IEEE Trans. Ultrason. Ferroelectrics Freq. Control 44 (1997) 1027–1037.
[32] D. Tortora, V. Panara, P.A. Mattei, et al., Comparing 3T T1-weighted sequences in identifying hyperintense punctate lesions in preterm neonates, AJNR Am J Neuroradiol 36 (2015) 581–586.
[33] M. Riccabona, Neonatal neurosonography, Eur. J. Radiol. 83 (2014) 1495–1506.
[34] J. Kurian, S. Sotardi, M.C. Liszewski, et al., Three-dimensional ultrasound of the neonatal brain: technical approach and spectrum of disease, Pediatr. Radiol. 47 (2017) 613–627.
[35] J.M. Romero, N. Madan, I. Betancur, et al., Time efficiency and diagnostic agreement of 2-D versus 3-D ultrasound acquisition of the neonatal brain, Ultrasound Med. Biol. 40 (2014) 1804–1809.
[36] Y.J. Kim, Y.H. Choi, H.H. Cho, et al., Comparison between 3-dimensional cranial ultrasonography and conventional 2-dimensional cranial ultrasonography in neonates: impact on reinterpretation, Ultrason Seoul Korea 37 (2018) 63–70.
[37] D.L. Harris, F.H. Bloomfield, R.L. Teele, et al., Variable interpretation of ultrasonograms may contribute to variation in the reported incidence of white matter damage between newborn intensive care units in New Zealand, Arch. Dis. Child. Fetal Neonatal Ed. 91 (2006) F11–F16.
[38] S.R. Hintz, T. Slovis, D. Bulas, et al., Interobserver reliability and accuracy of cranial ultrasound scanning interpretation in premature infants, J. Pediatr. 150 (2007), 592–6, 596.e1-5.
[39] S. Westra, I. Adler, D. Batton, et al., Reader variability in the use of diagnostic terms to describe white matter lesions seen on cranial scans of severely premature infants: the ELGAN study, J Clin Ultrasound JCU 38 (2010) 409–419.
[40] C.F. Hagmann, M. Halbherr, B. Koller, et al., Interobserver variability in assessment of cranial ultrasound in very preterm infants, J Neuroradiol J Neuroradiol 38 (2011) 291–297.